Second order nonlinear optical properties of poled films containing azobenzenes tailored with azulen-1-yl-pyridine

Ana-Maria Manea-Saghin [a,*], Adrian E. Ion [b], Francois Kajzar [a,c], Simona Nica [b,**]

[a] Faculty of Chemical Engineering and Biotechnologies, Research Center for Environmental Protection and Eco-friendly Technologies, University POLITEHNICA of Bucharest, Polizu Street No 1, 011061, Bucharest, Romania
[b] "C. D. Nenitzescu" Institute of Organic and Supramolecular Chemistry, Romanian Academy, Splaiul Independentei 202 B, 060023, Bucharest, Romania
[c] Laboratoire de Chimie, CNRS, Université Claude Bernard, ENS-Lyon, 46 Allée d'Italie, 69364 Lyon cedex 07, France

ARTICLE INFO

ABSTRACT

Azo compounds, which are highly versatile molecules, have attracted a considerable attention both for their fundamental properties and for practical applications, especially in photonics. The conjugated azo-aromatic systems containing 4-(R-azulen-1-yl)-2,6-dimethyl-pyridine were investigated for their nonlinear optical properties. These molecules were embedded in polymethyl methacrylate (PMMA) matrix, and the obtained guest-host systems were processed into good optical quality thin film by spin coating technique. The dipolar moments of dissolved in PMMA molecules were oriented by applying a high DC electric field at a temperature close to the polymer glass transition temperature. The second - order nonlinear optical (NLO) properties of poled films were studied by the optical second harmonic generation technique (SHG). The poling kinetics, studied by *in situ* SHG as well as the measured second-order NLO susceptibilities of poled films are reported and discussed.

1. Introduction

Organic materials possessing nonlinear optical (NLO) properties have attracted considerable attention in the last period due to their potential applications in state-of-the-art devices such as dye-sensitized solar cells [1,2], optical data storage devices [3,4], communications [5,6], two-photon fluorescence microscopes [7–9] and photodynamic therapy [10,11]. Due to their large nonlinear optical responses, the conjugated organic compounds containing both electron donor and acceptors widely known as push-pull compounds, have aroused great interest in the field of nonlinear optics. As a matter of fact, azobenzene and its functionalized compounds have been extensively used for construction of optical switching materials owing to their unique and clean photoisomerization [12,13]. Grafting various electron-donating or -accepting groups onto the molecular skeleton of azobenzenes, has been reported to successfully lead to NLO materials with increased nonlinearity [14]. In this regard, we expect that the investigation of the structure-property relationship of the substituted azobenzene derivatives will have a great impact in developing efficient molecular switches with direct application in optical signal processing or for optical data storage modules [15,16]. At the same time, employing azulene derivatives as precursors in designing electronic and optical materials, has attracted an increased attention owing to their unique fluorescent and redox properties

---

[17,18]. So far, this blue-colored hydrocarbon proved to be an attractive building block for developing molecular switches [19,20], liquid crystals [21,22], supramolecular assemblies [23,24], organic transistors [25], redox-active covalent organic framework [26], and high conductance materials [27]. A relevant characteristic of azulene in the construction of push-pull compounds is its dipole moment of about 1.08 D [28], arising from the electron drift from the seven-membered ring to its five-membered ring, leading to an intrinsic dipolar structure [29]. Owing to this peculiar feature, azulene can act either as electron donor or as electron acceptor and, moreover, as conjugated bridge in push-pull compounds [30].

Based on semi-empirical *ab initio* calculations we expect an NLO response of azulene comparable to well-established NLO-phores [31]. The first examples of azulene-based compounds possessing NLO properties, comprising of azulene or guaiazulene as donor groups, respectively, dicyanovinyl (**A,** Fig. 1) and 1,3-diethyl-2-thiobarbituric acid (**B,** Fig. 1) as acceptor groups, were reported by Asato et al. [32]. Following these examples, the potential of several azulene-based substituted pyiridinium cations (**C,** Fig. 1) [33] and azo-azulene derivatives (**D,** Fig. 1) [34–36] to behave as efficient NLO systems, has been confirmed. For example, in comparison to the commercially available Disperse Red One (**DR1,** Fig. 1) NLO chromophore [33], (4-nitrophenylazo)-azulene (**E,** Fig. 1) showed a larger β value, of about $80*10^{-30}$ cm^{-5} esu^{-1} (at 1.907 μm) [35]. Moreover, composite films containing azo-azulenes as phenyl-based (hydroxyphenyl, acetamidophenyl) or thiazole-based (thiazole and benzothiazole) chromophores showed an uncommon phenomenon of formation of photoinduced surface graftings produced by the photoisomerization of the azo bond [36]. Also, several (ferrocenylethynyl)azulenes [37] and highly substituted azulene dyes [38] have been identified as interesting NLO switches.

These results have encouraged us to investigate nonlinear optical properties of 4-(azulen-1-yl)-pyridines substituted at C3-position of azulene with mono-azobenzene derivatives. We have previously reported the straitforward synthesis of these highly conjugated azo-aromatic systems obtained from azulenyl pyridine coupled diazonium salts of substituted anilines [39]. The fluorescence emission above 530 nm displayed by these compounds is induced by the attachment of the azulenyl moiety to the azobenzene molecules and explained by the unusual $S_2 \rightarrow S_0$ azulene transition. In addition, upon exposure to UV light for a short period of time, the thermally stable *E* isomer was converted to the corresponding *Z* isomer, whereas exposure of the irradiated solutions to sunlight for a day caused the recovery of the stable isomer [40].

The current study reports on a comparative investigation regarding the second harmonic generation ability of highly conjugated azulenyl azo dyes doped in polymethyl methacrylate (PMMA) matrix. The molecular structure of the chromophores employed in the present study is presented in Scheme 1. Based on NLO properties, the main goal of this investigation was to determine the correlation between azulene derivatives and azo-benzene family in terms of second harmonic generation (SHG). The studied compounds differ in terms of azulen-substitution which is affecting the electron distribution cloud of the push-pull compounds and, thus, their NLO response. Samples were prepared as solid-state film blends with poly(methyl metacrylate) (PMMA) of various loadings of dye. To our knowledge, this is the first time when the second harmonic generation of azulene-derivatives in PPMA matrix is investigated.

2. Methodology

2.1. Material synthesis

Thin films containing four azulene based compounds were obtained by the spin-coating technique on glass substrate using a spin-
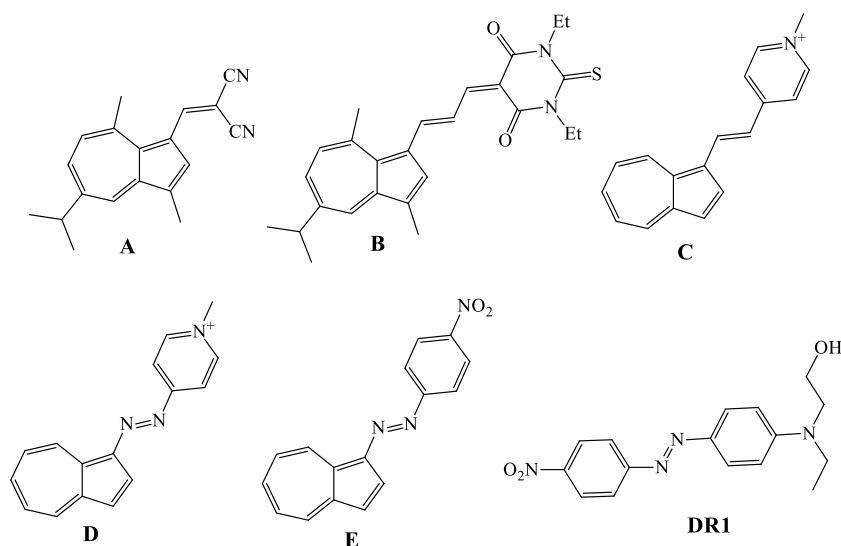

Fig. 1. Representative azulene-based NLO-phores; 2-((5-isopropyl-3,8-dimethylazulen-1-yl)methylene)malononitrile (A), (E)-1,3-diethyl-5-(3-(5-isopropyl-3,8-dimethylazulen-1-yl)allylidene)-2-thioxodihydropyrimidine-4,6(1H,5H)-dione (B), (E)-4-(2-(azulen-1-yl)vinyl)-1-methylpyridin-1-ium (C), (E)-4-(azulen-1-yldiazenyl)-1-methylpyridin-1-ium (D), (E)-1-(azulen-1-yl)-2-(4-nitrophenyl)diazene (E), (E)-2-(ethyl(4-((4-nitrophenyl)diazenyl)phenyl)amino)ethanol (DR1).
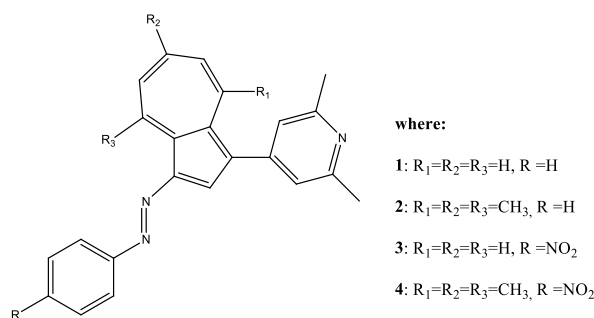
Scheme 1. Chemical structure of the compounds under investigation.

coater from Laurell Technologies Corporation, model WS-400B-6NPP/LITE. Then, the films were dried for 1 h at 70 °C to evacuate the remaining solvent. Their spectroscopic properties within UV-VIS range were characterized with the JASCO V560 spectrometer. The absorption spectra of the films are shown in Fig. 2. The thin films thicknesses were determined by the profilometry technique using DEKTAK 120 apparatus of KLA Tencor Company. The device allows the thickness measurement of each deposited film on a hard and smooth glass surface. Measurements were done in triplicate, and the values are listed in Table 1.

2.2. Spectral characterization

For the spectroscopic experiments, the series of thin polymeric films for each of the investigated compounds was prepared as follows. We used commercially available poly(methyl methacrylate) (Mw ¼ 966 kDa, Sigma Aldrich®) in powder form and the family of the 4-(azulen-1-yl)-pyridine derivatives [39] is shown in Scheme 1. First, solutions of PMMA/TCE in T2, 5 and 10% ratios were prepared. After mixing and heating for few days, when the polymer completely dissolved, we mixed the above mentioned solutions to obtain the final mixture (3% dry weight proportion between the 4-(azulen-1-yl)-pyridine derivative and polymer) of a simple guest-host system, where the active material is stabilized by a branched, well-defined, transparent, and high laser damage threshold polymer matrix [41]. After stirring and heating, the final solution (azulenylpyridine/PMMA/TCE) was deposited on a clean silica glass plate using the spin-coating technique. The layers were dried at 70 °C to evaporate the remaining solvent. The measured with Tencor,
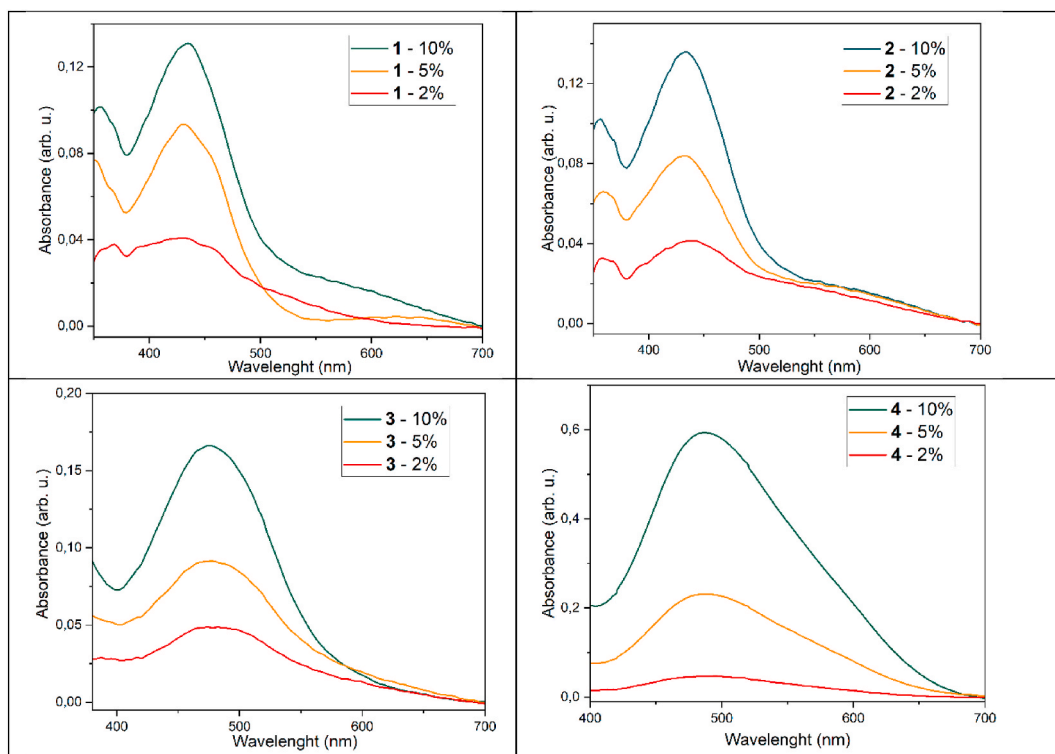

Fig. 2. Absorption spectra of the investigated azulenylpyrydine-azo dyes, **1**–**4** in PMMA films.

Table 1

Dye concentration, film thickness and maximum absorption wavelength λ_{max} of investigated azulenylpyrydine-azo dyes in PMMA films.

Compound	Concentration (w%)	Thickness (nm)	Absorption maxima (nm)
1	2	394.6	433
	5	327.8	430
	10	357.1	431
2	2	255.3	432
	5	280.2	433
	10	292.1	433
3	2	252.8	474
	5	272.2	476
	10	287.3	476
4	2	310.7	485
	5	621.3	486
	10	903.8	487

ALFA-Step profilometer thicknesses of the studied films are presented in Table 1.

2.3. The film poling and second second-order NLO properties characterization

The spin-coating method used for thin film fabrication technique leads to obtaining centrosymmetric materials with no second order NLO properties, albeit the constituent guest molecules are noncentrosymmetric. This one can be obtained by applying a high intensity DC field to the film which orient the dipolar moments mostly in its direction. This was got by corona poling (CP (method) discharge charge deposition on the thin film surface. The applied voltage was of *ca.* 6 kV. More details can be found in Refs. [42,43].

The electric field poling can be performed at every temperature. However, its rate and speed depend on the molecules rotational mobility, which depends on temperature. Usually poling is done close, but a little below the glass transition temperature. In our case it was done at ca 96 °C with polymer Tg of 97 °C. The poling process takes *ca* 5 min, and its kinetics is followed by the *in situ* SHG measurements (cf refs. [42,43]. After it, the poled film is cooled to the ambient temperature under the applied CP field to fix the created polar order.

The second order NLO susceptibility $\chi^{(2)}(-2\omega; \omega, \omega)$ of studied films was measured in infrared (1064.2 nm) by the second harmonic generation (SHG) method, collecting the generated 532 nm wave intensity as function of the incidence angle θ. The used for that light source is a Nd:YAG laser operating with 10 Hz frequency and 6 ns pulse duration. The data are calibrated by the SHG measurements on an α-quartz single crystal, done at the same conditions (for details see Ref. [42]).

Thin film fabrication by solution spinning on substrates coating leads to centrosymmetric thin films with SHG susceptibility $\chi^{(2)}_{IJK}(-2\omega; \omega, \omega) \equiv 0$ for all its components I, J, K. Thus, to get this property it is necessary to create noncentrosymmetry. One of the ways to do it is application of the DC electric field. As the molecules used are forcibly noncentrosymmetric they possess a dipole moment. Its interaction with the applied electric field orients them in its direction, creating noncentrosymmetry. The point symmetry of an electric field poled film is ∞mm with two meaningful $\chi^{(2)}(-2\omega; \omega, \omega)$ components: the diagonal $\chi^{(2)}_{ZZZ}(-2\omega; \omega, \omega)$ and the off diagonal $\chi^{(2)}_{XXZ}(-2\omega; \omega, \omega)$, where Z is the poling field direction. Components, which are material property parameter are measured by an appropriate choice of polarization of fundamental (f) and harmonic (h) beams.

As it is usually done with the harmonic generation methods the NLO tensor components were determined by an appropriate choice of the incident fundamental *(b)* and the outgoing harmonic (h) beams polarizations. The intensity of the generated harmonic wave as function of the incidence angle θ is given by [42,44]

$$I^{bh}_{2\omega}(\theta) = \frac{32\pi^3}{c^2} \left| \frac{\chi^{(2)}_{bbh}(-2\omega; \omega, \omega)}{\Delta\varepsilon} \right|^2 |T_{bh}(\theta)A_{bh}(\theta)|^2 \left| e^{i\Delta f_{bbh}} - 1 \right|^2 I^2_\omega \tag{1}$$

where c denotes the light speed, $T_{bh}(\theta)$ and $A_{bh}(\theta)$ are factors arising from the transmission and boundary conditions for the propagating fundamental and harmonic beams (for details see Ref. [44]).

I_ω in Eq. (1) is the fundamental beam intensity and $\Delta\varepsilon$ is the dielectric constant mismatch between the fundamental (ω) and the harmonic (2ω) [42] frequencies.

$$\Delta\varepsilon = \varepsilon(2\omega) - \varepsilon(\omega) \tag{2}$$

The phase mismatch Δf between the propagating fundamental and the harmonic beams in Eq. (1) is given by [42]

$$\Delta f_{bh} = \varphi^b(\omega) - \varphi^h(2\omega) = \frac{4\pi l}{\lambda_\omega} \left(n^b_\omega \cos\theta^b_\omega - n^h_{2\omega} \cos\theta^h_{2\omega} \right) \tag{3}$$

where φ^b_ω and $\varphi^h_{2\omega}$ are, respectively, fundamental ω and harmonic 2ω frequency beams phases. In a similar manner θ^b_ω and $\theta^h_{2\omega}$) are their propagation angles. l in Eq. (3) denotes the studied thin film thickness.

In practice the SHG measurements are performed in p-p polarization configuration, taking the ratio $\chi^{(2)}_{XXZ}(-2\omega; \omega, \omega)/\chi^{(2)}_{ZZZ}(-2\omega; \omega,$
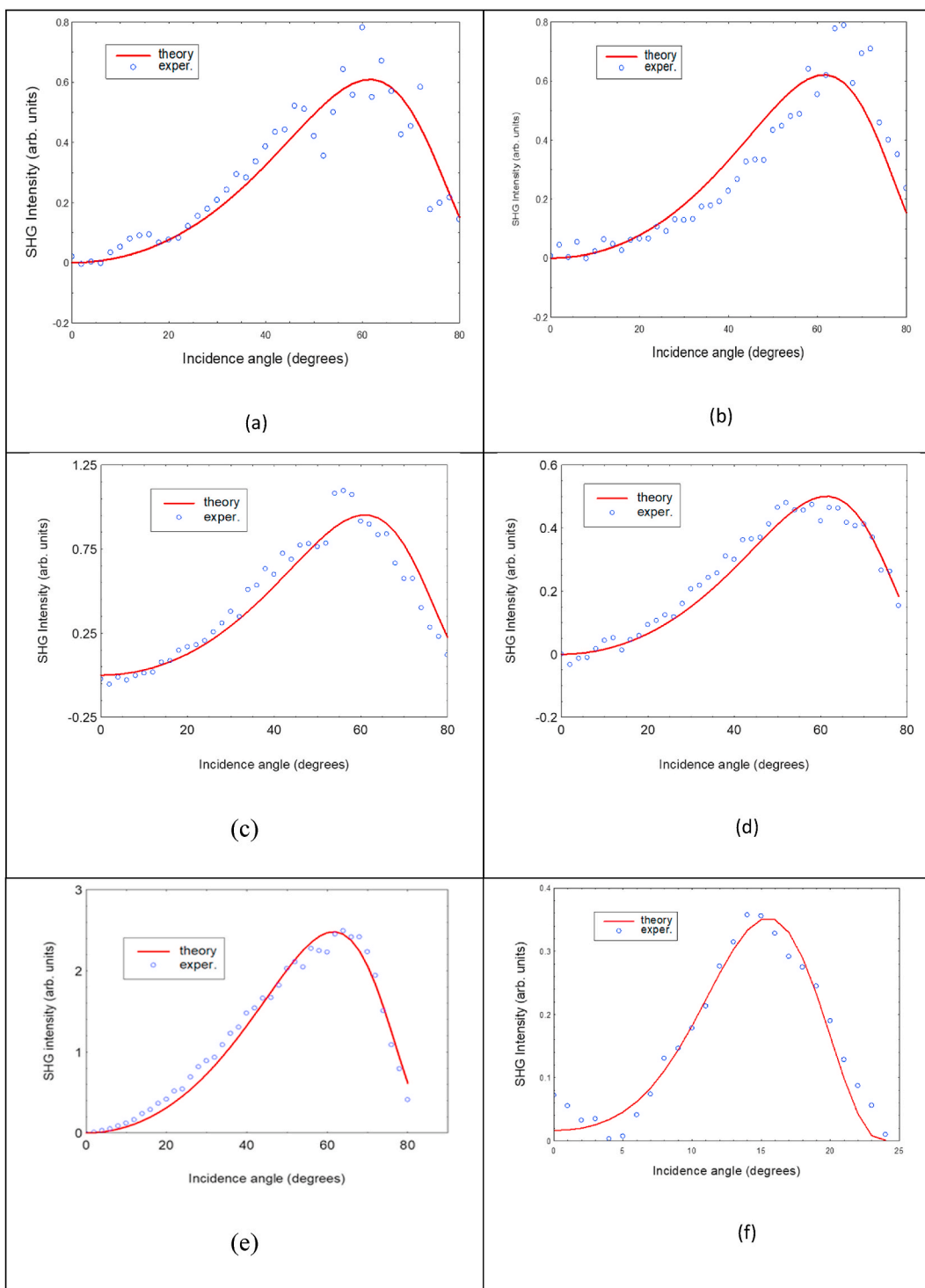
Fig. 3. Incidence angle dependence of SHG intensity for a poled thin films (a–d) and for an α-single crystal quartz plate used for calibration (e–f). Points are measured values whereas solid lines depicts the calculated ones.

$\omega) = 1/3$, as predicted by the free electron model. In that case the effective quadratic susceptibility to insert in Eq (1) is given by Refs. [42,44–46,].

$$\chi_{ppp}^{(2)}(-2\omega, \omega, \omega) = \chi_{ZZZ}^{(2)} \left[\sin^2\theta_\omega^p \sin\theta_{2\omega}^p + \frac{1}{3} \left(\cos\theta_\omega^p \left(\cos\theta_\omega^p + 2\sin\theta_\omega^p \cos\theta_{2\omega}^p \right) \right) \right] \tag{4}$$

for p-p fundamental-harmonic beams polarization configurations.

Eq. (1) with inserted Eqs. (2)–(4) describes the actual variation of the SHG intensity for this polarization configuration. So modified formula was used to fit the experimental SHG spectra for the studied films. Fig. 3 shows both the measured (points) and fitted values. Similar procedure was applied for SHG measurements on an $\alpha-$quartz plate, done at the same condition and used for calibration of the studied thin film values. An example of a fit of SHG spectra for a quartz play is displayed in Fig. 3(f). Comparing the fitting parameters for studied films and for quartz one gets the actual value of $\chi_{ZZZ}^{(2)}(-2\omega; \omega, \omega)$ susceptibility for the studied material.

3. Results and discussions

3.1. Molecules synthesis, thin films preparation and optical spectroscopy

The investigated compounds were synthesized as previously described [39] through azo-coupling reaction of 4-azulenylpyridines with the diazonium salts of anilines, in potassium acetate buffer. The reactions proceed in mild conditions with moderate to high yields, making the compounds easily accessible. All of the investigated compounds present strong absorption bands in thin film form prepared using polymethyl-methacrylate (PMMA) polymeric matrix. The solutions were obtained by dissolving, under stirring, the host (PMMA) and guests (azulenylpyridine-azo dyes) molecules in 1,1,2 trichloroethane (TCE) by heating for few days, until the polymer was completely dissolved. The final solution (azulenylpyridine dye/PMMA/TCE) was deposited on a clean silica glass plate using the spin coating technique. The layers were dried at 70 °C until the evaporation process was finished. There were used solutions with three different concentrations of each of the four chromophores (2, 5 and 10 w %). The thickness of the studied films was measured with profilometer, and the data are given in Table 1.

The maximum absorption wavelength λ_{max} of the azo-benzene substituted 4-azulenylpyridine in PMMA film is located at around 437 nm. In solution, the dye λ_{max} is 425 nm, with small influence of the solvent polarity on the maximum absorption wavelength [39, 40]. It is worth mentioning that putting the pyridine moiety on the azo-azulene push-pull system for extension of the electron conjugation path, does not cause a significant change λ_{max} as compared to azoazulene derivatives [36]. The azulene substitution results in a little extend of the position of the absorbtion maxima position, whereas introduction of the electron withdrawing group in azobenzene moiety causes a significant red shift of the absorption band. The absorption spectrum of compound **2** shows a λ_{max} at 440 nm in PMMA film (Fig. 2). Instead, the absorption maxima for the molecules possessing $-NO_2$ substituent at the para-position of the azobenzene unit are red-shifted and are positioned at 497 (compound **3**) and 499 nm (compound **4**), respectively.

3.2. Second order nonlinear optical properties

The SHG efficiency of the films was investigated using our previously reported technique [42,43], by measuring the SHG intensities as a function of the incidence angle. Thus, the set-up supposed the rotation of the studied film along the axis perpendicular to the direction of the beam propagation which coincides with the p polarization of the used incident and harmonic waves. Circles show the measured while the continuous lines the fitted values using Eq. (1) harmonic intensities. A very good agreement is observed.

Fig. 3 (a – f) shows the observed, typical, dependence of SHG intensity on incidence angle for studied films and for α-quartz thin crystal plate used for calibration. At normal incidence $I_{2\omega}$ is null because the fundamental beam polarization is perpendicular to the molecule dipole moment. It can be observed that, the SHG intensity increases with the increase of θ values, reaching a maximum for θ

Table 2
Second-order NLO susceptibility of studied materials at 1064.2 nm fundamental wavelength.

Compound	Concentration (w%)	$\chi_{ZZZ}^{(2)}(-2\omega, \omega, \omega)$
1	2	2.6
	5	5.4
	10	7.2
2	2	3.5
	5	3.5
	10	5.4
3	2	21.7
	5	28.3
	10	37.5
4	2	11.6
	5	14.8
	10	32.3
$\alpha-$quartz [47]		1
LiNbO$_3$ [52]		25.2

$= 90°$. Due to the increasing reflection with the increase of the incidence angle, less light is coupled into thin film because it competes with the mentioned increase due to the decreasing angle between electric field and dipole moment direction. As a result, the SHG intensity, after reaching a maximum, decreases, up to zero at $\theta = 180°$. In the SHG measurements the fundamental beam fluctuations are considered by measuring the intensity of reflected, very small part of fundamental beam with a fast photodetector and correcting for [42]. The optical absorption of studied films was taken into account by using complex refractive indices in Eq. (1).

As mentioned, the SHG susceptibilities of the studied films were calibrated by SHG measurements on a α-quartz single crystal plate, in the same conditions. Fig. 3(e) shows an example of such measurements, performed also in p-p fundamental – harmonic field polarization configuration. Because the quartz data were used for calibration, they were also fitted using the well-established formula [42]. An excellent agreement can be observed as it is shown in Fig. 3(f). The derived in this way diagonal $\chi^{(2)}_{ZZZ}(-2\omega; \omega, \omega)$ susceptibility tensor component for the studied films with dopant concentrations: 2, 5 and 10 w% are listed in Table 2. They were calibrated using for the α-quartz single crystal $\chi^{(2)}_{ZZZ}(-2\omega; \omega, \omega) = 1$ p.m./V as determined by Choy and Byer [47]. The data listed in Table 2 show that molecules (**1**, **2**) with lowest $\lambda_{\max}$ exhibit significantly smaller $\chi^{(2)}_{ZZZ}(-2\omega; \omega, \omega)$ susceptibilities than the more conjugated ones (**3**, **4**). This is in accordance with the reported dependence (see e.g. Kajzar [48]) of the NLO susceptibilities on the π electron conjugation length. There is another factor which leads to higher NLO susceptibilities of molecules (**3**, **4**) too, namely the two photon resonance contribution. For both of them $\lambda_{\max}$ is closer to the second harmonic wavelength of 532.1 nm than for (**1**, **2**). One can also observe that in all cases, the NLO susceptibility doesn't vary linearly with the concentration, as expected. This is a characteristic feature of the π electron conjugated charge transfer molecules, which usually possess a large ground state dipole moment. Although it is beneficiary for the electric field poling efficiency, it is highly unwanted for potential application of these materials in NLO devices. The strong dipole – dipole interaction results in the formation of centrosymmetric aggregates, with no second order NLO response [49]. As consequence of the aggregation, the second order NLO susceptibility of the material stops increasing proportionally with the concentration of NLO molecules or even its decrease [50,51]. Moreover, the aggregates scatter light, increasing, often significantly, the light propagation losses in material.

The largest values of $\chi^{(2)}_{ZZZ}(-2\omega; \omega, \omega)$ observed for molecules **3** & **4** (37.5 and 32.3 p.m./V, respectively) compare favorably with that of the reference material LiNbO$_3$ single crystal (25.2 p.m./V [4]), but smaller than pyrazole-containing push-pull compounds [43] or Disperse Red One (DR1) NLO chromophore [53].

4. Conclusions

A series of π electron conjugated, noncentrosymmetric azo-aromatic molecules tailored with azulen-1-yl-pyridine were investigated for their nonlinear optical properties. For this purpose, the azobenzenes containing 4-(R-azulen-1-yl)-2,6-dimethyl-pyridine (R═H, –CH$_3$) were dissolved in polymethyl methacrylate to obtain solid thin films through spin-coating technique. In all cases, the PMMA thin films containing the investigated chromophores showed strong absorption band in the visible region. The films can be poled giving NLO materials with the diagonal $\chi^{(2)}_{ZZZ}(-2\omega; \omega, \omega)$ susceptibility, depending on concentration, spanning between 2.6 and 37.5 p.m./V at 1064.2 nm. For the most concentrated samples **3** and **4** with 10 w % guest concentration, the measured $\chi^{(2)}_{ZZZ}(-2\omega; \omega, \omega)$ susceptibilties of 37.5 and 32.3 p.m./V compare favorably to that of the reference LiNbO$_3$ single crystal (25.2 p.m./V [49]). A direct comparison with (4-nitrophenylazo)-azulene, reported as good NLOphore [35] can not be made now, since the reported hyperpolarizability was investigated using different experimental set-up.

Author contribution statement

Ana-Maria Manea-Saghin: Conceptualization, Visualization, Methodology, Investigation, Writing - Original Draft, Writing - Review & Editing, Supervision.

Adrian E. Ion: Investigation, Methodology, Formal analysis, Data Curation.

François Kajzar: Supervision, Writing - Review & Editing.

Simona Nica: Conceptualization, Investigation, Methodology, Data Curation, Writing - Original Draft, Writing - Review & Editing.

Funding statement

Data availability statement

No data was used for the research described in the article.

Declaration of competing interest

The authors declare that they have no known competing financial interests or personal relationships that could have appeared to influence the work reported in this paper.

References

[1] G. Boschloo, Improving the performance of dye-sensitized solar cells, Front. Chem. 7 (2019) 77, https://doi.org/10.3389/fchem.2019.00077.

[2] C.-P. Lee, C.-T. Li, K.-C. Ho, Use of organic materials in dye-sensitized solar cells, Mater. Today 20 (2017) 267–283, https://doi.org/10.1016/j.mattod.2017.01.012.

[3] L. Zhou, J. Mao, Y. Ren, S.-T. Han, V.A.L. Roy, Y. Zhou, Recent advances of flexible data storage devices based on organic nanoscaled materials, Small 14 (2018) 1703126, https://doi.org/10.1002/smll.201703126.

[4] K. Ogawa, Two-photon absorbing molecules as potential materials for 3D optical memory, Appl. Sci. 4 (2014) 1–18, https://doi.org/10.3390/app4010001.

[5] M.G. Papadopoulos, A.J. Sadlej, J. Leszczynski, Non-linear Optical Properties of Matter: from Molecules to Condensed Phases NLO Properties, Springer, 2006, 10:9781402048494.

[6] C.W. Ghanavatkar, V.R. Mishra, S. Nagaiyan, Review of NLOphoric azo dyes – developments in hyperpolarizabilities in last two decades, Dyes Pigments 191 (2021), 109367, https://doi.org/10.1016/j.dyepig.2021.109367.

[7] R. Li, Y. Zhang, X. Xu, Y. Zhou, M. Chen, M. Sun, Optical characterizations of two-dimensional materials using nonlinear optical microscopies of CARS, TPEF, and SHG, Nanophotonics 7 (2018) 873–888, https://doi.org/10.1515/nanoph-2018-0002.

[8] X. Mi, Y. Wang, R. Li, M. Sun, Z. Zhang, H. Zheng, Multiple surface plasmon resonances enhanced non-linear optical microscopy, Nanophotonics 8 (2019) 487–493, https://doi.org/10.1515/nanoph-2018-0231.

[9] L. Xu, J. Zhang, L. Yin, X. Long, W. Zhang, Q. Zhang, Recent progress in efficient organic two-photon dyes for fluorescence imaging and photodynamic therapy, J. Mater. Chem. C 8 (2020) 6342–6349, https://doi.org/10.1039/D0TC00563K.

[10] Y. Shen, A.J. Shuhendler, D. Ye, J. Jing, H. Chen, Two-photon excitation nanoparticles for photodynamic therapy, Chem. Soc. Rev. 45 (2016) 6725–6741. https://pubs.rsc.org/en/content/articlelanding/2016/CS/C6CS00442C.

[11] L.K. McKenzie, H.E. Bryant, J.A. Weinstein, Transition metal complexes as photosensitisers in one-and two-photon photodynamic therapy, Coord. Chem. Rev. 379 (2019) 2–29, https://doi.org/10.1016/j.ccr.2018.03.020.

[12] H.M.D. Bandara, S.C. Burdette, Photoisomerization in different classes of azobenzene, Chem. Soc. Rev. 41 (2012) 1809–1825, https://doi.org/10.1039/C1CS15179G.

[13] A.B. Grommet, L.M. Lee, R. Klajn, Molecular photoswitching in confined spaces, Acc. Chem. Res. 53 (2020) 2600–2610, https://doi.org/10.1021/acs.accounts.0c00434.

[14] A. Fihey, A. Perrier, W.R. Browne, D. Jacquemin, Multiphotochromic molecular systems, Chem. Soc. Rev. 44 (2015) 3719–3759, https://doi.org/10.1039/C5CS00137D.

[15] F. Zhao, L. Grubert, S. Hecht, D. Bléger, Orthogonal switching in four-state azobenzene mixed-dimers, Chem. Commun. 53 (2017) 3323–3326, https://doi.org/10.1039/C7CC00504K.

[16] K. Kuntze, J. Isokuortti, A. Siiskonen, N. Durandin, T. Laaksonen, A. Priimagi, Azobenzene photoswitching with near-infrared light mediated by molecular oxygen, J. Phys. Chem. B 125 (2021) 12568–12573, https://doi.org/10.1021/acs.jpcb.1c08012.

[17] G. Eber, F. Grüneis, S. Schnider, F. Dörr, Dual fluorescence emission of azulene derivatives in solution, Chem. Phys. Lett. 29 (1974) 397–404, https://doi.org/10.1016/0009-2614(74)85131-6.

[18] A.E. Ion, L. Cristian, M. Voicescu, M. Bangesh, A.M. Madalan, D. Balea, C. Mihailciuc, S. Nica, Synthesis and properties of fluorescent 4′-azulenyl-functionalized 2,2′:6′,2″-terpyridines, Beilstein J. Org. Chem. 12 (2016) 1812–1825, https://doi.org/10.3762/bjoc.12.171.

[19] E.A. Dragu, A.E. Ion, S. Shova, D. Bala, C. Mihailciuc, S. Ionescu, S. Nica, Visible-light triggered photoswitching systems based on fluorescent azulenyl-substituted dithienylcyclopentenes, RSC Adv. 5 (2015) 63282–63286, https://doi.org/10.1039/C5RA11974J.

[20] I.C.-Y. Hou, F. Berger, A. Narita, K. Müllen, S. Hecht, Proton-gated ring-closure of a negative photochromic azulene-based diarylethene, Angew. Chem., Int. Ed. 59 (2020) 18532–18536, https://doi.org/10.1002/anie.202007989.

[21] K. Nakagawa, T. Yokoyama, K. Toyota, N. Morita, S. Ito, S. Tahata, M. Ueda, J. Kawakami, M. Yokoyama, Y. Kanai, K. Ohta, Synthesis and liquid crystalline behavior of azulene-based liquid crystals with 6-hexadecyl substituents on each azulene ring, Tetrahedron 66 (66) (2010) 8304–8312, https://doi.org/10.1016/j.tet.2010.08.012.

[22] A.U. Petersen, M. Jevric, R.J. Mandle, M. T Sims, J. N Moore, S.J. Cowling, J.W. Goodby, M.B. Nielsen, Photoswitching of dihydroazulene derivatives in liquid-crystalline host systems, Chem. Eur J. 23 (2017) 5090–5103.

[23] A. E Ion, A. Dogaru, S. Shova, A.M. Madalan, O. Akintola, S. Ionescu, M. Voicescu, S. Nica, A. Buchholz, W. Plass, M. Andruh, Organic co-crystals of 1,3-bis(4-pyridyl)azulene with a series of hydrogen-bond donors, CrystEngComm 20 (2018) 4463–4484, https://doi.org/10.1039/C8CE00945G.

[24] A.E. Ion, S. Nica, A.M. Madalan, C. Maxim, M. Julve, F. Lloret, M. Andruh, One-dimensional coordination polymers constructed from di-and trinuclear {3d–4f} tectons. A new useful spacer in crystal engineering: 1,3-bis (4-pyridyl) azulene, CrystEngComm 16 (2014) 319–327, https://doi.org/10.1039/C3CE41592A.

[25] H. Katagiri, Azulene-based materials for organic field-effect transistors, in: M. Sakamoto, H. Uekusa (Eds.), Advances in Organic Crystal Chemistry, Springer, Singapore, 2020, https://doi.org/10.1007/978-981-15-5085-0_17.

[26] Z. Zhao, M.E. El-Khouly, Q. Che, F. Sun, B. Zhang, H. He, Y. Chen, Redox-active azulene-based 2D conjugated covalent organic gramework for organic memristors, 202217249, Angew. Chem., Int. Ed. (2023), https://doi.org/10.1002/anie.202217249.

[27] H. Gao, C. Ge, B. Hou, H. Xin, X. Gao, Incorporation of 1,3-free-2,6-connected azulene units into the backbone of conjugated polymers: improving proton responsiveness and electrical conductivity, ACS Macro Lett. 8 (2019) 360–1364, https://doi.org/10.1021/acsmacrolett.9b00657.

[28] A. Murakami, T. Kobayashi, A. Goldberg, S. Nakamur, CASSCF and CASPT2 studies on the structures, transition energies, and dipole moments of ground and excited states for azulene, J. Chem. Phys. 120 (2004) 1245–1252, https://doi.org/10.1063/1.1631914.

[29] K.-P. Zeller, in: H. Kropf (Ed.), Houben Weyl, Methoden der Organischen Chemie, vol. V, Georg Thieme Verlag, Stuttgart, Germany, 1985, pp. 127–418.

[30] L. Huang, N. Eedugurala, A. Benasco, S. Zhang, K.S. Mayer, D.J. Adams, B. Fowler, M.M. Lockart, M. Saghayezhian, H. Tahir, E.R. King, S. Morgan, M.K. Bowman, X. Gu, J.D. Azoulay, Open-shell donor–acceptor conjugated polymers with high electrical conductivity, Adv. Funct. Mater. 30 (2020), 1909805, https://doi.org/10.1002/adfm.201909805.

[31] J.O. Morley, Nonlinear optical properties of organic molecules. 7. Calculated hyperpolarizabilities of azulenes and sesquifulvalene, J. Am. Chem. Soc. 110 (1988) 7660–7663, https://doi.org/10.1021/ja00231a013.

[32] A.E. Asato, R.S.H. Liu, V.P. Rao, Y.M. Cai, Azulene-containing donor-acceptor compounds as second-order nonlinear chromophores, Tetrahedron Lett. 37 (1996) 419–422, https://doi.org/10.1016/0040-4039(95)02202-3.

[33] L. Cristian, I. Sasaki, P.G. Lacroix, B. Donnadieu, I Asselberghs, K. Clays, A.C. Razus, Donating strength of azulene in various azulen-1-yl-substituted cationic dyes: application in nonlinear optics, Chem. Mater. 16 (2004) 3543–35551, https://doi.org/10.1021/cm0492989.

[34] J. Niziol, Z. Essaidi, H.E. Ouazzani, M. Bakasse, B. Sahraoui, Nonlinear optical properties of azo-azulenes derivatives, in: 12th International Conference on Transparent Optical Networks 2010, 2010, pp. 1–4, https://doi.org/10.1109/ICTON.2010.5549152.

[35] Z. Essaidi, J. Niziol, B. Sahraoui, Azo-azulene based compounds-nonlinear optical and photorefractive properties, Opt. Mater. 33 (2011) 1387–1390, https://doi.org/10.1016/j.optmat.2011.02.039.

[36] P.G. Lacroix, I. Malfant, G. Iftime, A.C. Razus, K. Nakatani, J.A. Delaire, Azo-azulene derivatives as second-order nonlinear optical chromophores, Chem. Eur J. 6 (2000) 2599–2608, https://doi.org/10.1002/1521-3765(20000717)6:14<2599::AID-CHEM2599>3.0.CO;2.

[37] T. Farrell, T. Meyer-Friedrichsen, M. Malessa, D. Haase, W. Saak, I. Asselberghs, K. Wostyn, K. Clays, A. Persoons, J. Heck, A.R. Manning, Azulenylium and guaiazulenylium cations as novel accepting moieties in extended sesquifulvalene type D–π–A NLO chromophores, J. Chem. Soc. Dalton Trans. 1 (2001) 29–36, https://doi.org/10.1039/B006624I.

[38] J. Huang, S. Huang, Y. Zhao, B. Feng, K. Jiang, S. Sun, C. Ke, E. Kymakis, X. Zhuang, Azulene-based molecules, polymers, and frameworks for optoelectronic and energy applications, Small Methods 4 (2020), 2000628, https://doi.org/10.1002/smtd.202000628.

[39] A.C. Razus, S. Nica, L. Cristian, M. Raicopol, L. Birzan, A.E. Dragu, Synthesis and physico-chemical properties of highly conjugated azo-aromatic systems. 4-(azulen-1-yl)-pyridines with mono- and bis azo-aromatic moieties at C3-position of azulene, Dyes Pigments 91 (2011) 55–61, https://doi.org/10.1016/j.dyepig.2011.02.008.

[40] E.A. Dragu, A. Hanganu, I. Rau, F. Kajzar, A. Tane, A.C. Razus, S. Nica, Photochemistry of fluorescent azobenzenes substituted with azulenylpyridine moiety, Mol. Cryst. Liq. Cryst. 604 (2014) 41–51, https://doi.org/10.1080/15421406.2014.967653.

[41] M. Moldoveanu, A. Meghea, R. Popescu, J.G. Grote, F. Kajzar, I. Rau, On the stability and degradation of dna based thin films, Mol. Cryst. Liq. Cryst. 522 (2010) 182–190, https://doi.org/10.1080/15421401003723086.

[42] I. Rau, F. Kajzar, Second harmonic generation and its applications, Nonl. Opt. Quant. Opt. 38 (2008) 99–140.

[43] A.-M. Manea, I. Rau, A. Tane, F. Kajzar, L. Sznitko, A. Miniewicz, Poling kinetics and second order NLO properties of DCNP doped PMMA based thin film, Opt. Mater. 36 (2013) 69–74, https://doi.org/10.1016/j.optmat.2013.05.012.

[44] J.D. Swalen, F. Kajzar, in: F. Kajzar, J.D. Swalen (Eds.), Introduction in Organic Thin Films for Waveguiding Nonlinear Optics, Gordon and Breach Publishers, Amsterdam, Philadelphia, Paris, 1996, pp. 289–327.

[45] K.D., Singer, M.D. Kuzyk, J.E. Sohn, Orientationally ordered electro-optic materials, in: P.N. Prasad, D.R. Ulrich (Eds.), Nonlinear Optical and Electroactive Polymers, Plenum Press, New York, 1988, pp. 189–204.

[46] K.D. Singer, J.E. Sohn, S.J. Lalama, Second harmonic generation in poled polymer films, Appl. Phys. Lett. 49 (1986) 248–250, https://doi.org/10.1063/1.97184.

[47] M.M. Choy, R.L. Byer, Accurate second-order susceptibility measurements of visible and infrared nonlinear crystals, Phys. Rev. B 14 (1976) 1693–1706, https://doi.org/10.1103/PhysRevB.14.1693.

[48] F. Kajzar, Impact of dimensionality, conjugation length, scaling laws and electronic structure on nonlinear optical properties of conjugated polymers, Nonl. Optics 5 (1993) 329–338.

[49] I. Rau, P. Armatys, P.-A. Chollet, F. Kajzar, Y. Bretonnière, C. Andraud, Aggregation: a new mechanism of relaxation of polar order in electro-optic polymers, Chem. Phys. Lett. 442 (2007) 329–333, https://doi.org/10.1016/j.cplett.2007.05.058.

[50] A.W. Harper, S.S. Sun, L.R. Dalton, S.M. Garner, A. Chen, S. Kalluri, W.H. Steier, B.H. Robinson, Translating microscopic optical nonlinearity to macroscopic optical nonlinearity: the role of chromophore electrostatic interactions, J. Opt. Soc. Am. B 15 (1998) 329–337, https://doi.org/10.1364/JOSAB.15.000329.

[51] G. Pawlik, I. Rau, F. Kajzar, A.C. Mitus, Second–harmonic generation in poled polymers: pre–poling history paradigm, Opt Express 18 (2010) 18793–18804, https://doi.org/10.1364/OE.18.018793.

[52] I. Shoji, T. Kondo, A. Kitamoto, M. Shirane, R. Ito, Absolute scale of second-order nonlinear-optical coefficients, J. Opt. Soc. Am. B 14 (1997) 2268–2294, https://doi.org/10.1364/JOSAB.14.002268.

[53] S.K. Yesodhaa, C.K.S. Pillaia, N. Tsutsumi, Stable polymeric materials for nonlinear optics: a review based on azobenzene systems, Prog. Polym. Sci. 29 (2004) 45–74. https://doi:10.1016/j.progpolymsci.2003.07.002.